Conformation of Uncomplexed Polyether Macrocycles. The Structure of Bis(2'-carboxy-1',3'-xylyl)-24-crown-6* at 113 K

By Israel Goldberg

Institute of Chemistry, Tel-Aviv University, Tel Aviv, Israel

Abstract

$C_{26}H_{32}O_{10}$ [bis(2'-carboxy-1',3'-xylyl)-24-crown-6] is orthorhombic, space group *Ccca* with $Z = 4$. At 113 K $a = 21 \cdot 405$ (5), $b = 12 \cdot 925$ (2), $c = 8 \cdot 878$ (3) Å. Final $R = 0 \cdot 045$ for 1098 low-temperature observations with $0 \cdot 50 \leq \sin \theta/\lambda < 0 \cdot 81$ Å^{-1} ($R = 0 \cdot 043$ for all 1660 data above threshold). The molecule has D_2 symmetry and an energetically favorable conformation. The macrocyclic framework accommodates an intramolecular carboxy dimer in which the O and H atoms are disordered. Intermolecular arrangement is stabilized by stacking forces between phenyl rings as well as by two-dimensional arrays of C—H⋯O attractions.

Introduction

The conformation of uncomplexed crown ether macrocycles in ordered crystal structures has been found to be determined primarily by intramolecular hydrogen bonds and transannular C—H⋯O attractions; in the absence of stabilizing interactions of a specific nature the empty molecules are usually disordered in the crystal even at low temperatures (Goldberg, 1980). It seemed reasonable, therefore, that incorporation of convergent functional groups into crown ether rings should have an influence on the stability of the ligand structure. In preceding papers we discussed the geometry of intramolecular interactions in two model compounds containing one 2-carboxy-1,3-xylyl unit as part of the polyether ring: 2,6-dimethylylbenzoic acid-18-crown-5 (Goldberg, 1976; referred to hereafter as BACR5) and 2,6-dimethylylbenzoic acid–2,6-dimethylylpyridine-18-crown-5 (Goldberg & Rezmovitz, 1978; referred to hereafter as BAPCR5). In both structures the carboxyl group is directed toward the center of the molecule, and hydrogen bonded to a transannularly located O (in BACR5) or N atom (in BAPCR5) nucleophile. As a result, the molecules have a lipophilic periphery, their arrangement in the crystal being effected mainly by ordinary van der Waals forces. Such packing is unusual in view of previous observations that monocarboxylic acids almost invariably form hydrogen-bonded carboxy dimers in the solid (Leiserowitz, 1976). The lipophilizing effect of a crown ether cavity is expected to be even more pronounced in bis(2'-carboxy-1',3'-xylyl)-24-crown-6 (I).
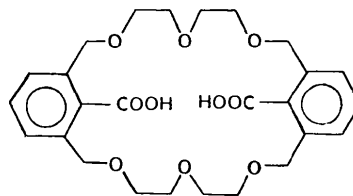
(I)

It can be seen from molecular models that the 24-membered ring in this ligand has almost ideal dimensions for an undistorted accommodation of a dicarboxyl pair. Moreover, it also provides an identical intramolecular environment for the carbonyl and hydroxyl O atoms. We describe below the crystal and molecular structures of this compound, and correlate its intra- and intermolecular topographic features with previously reported results for related species.

Experimental and structure determination

A crystal $0 \cdot 45 \times 0 \cdot 35 \times 0 \cdot 20$ mm was selected for the analysis. To obtain more precise structural parameters the diffraction experiment was carried out at 113 ± 5 K, the low temperature being maintained by a cooling apparatus designed by Strouse (1976). Accurate cell constants were determined by least squares from the setting angles of 15 reflections centered on a Syntex $P\bar{1}$ diffractometer. Crystal data are given in Table 1. Intensities were collected in the ω–2θ mode with graphite-crystal-monochromatized Mo K radiation ($\lambda = 0 \cdot 71069$ Å). 2715 unique reflections were recorded out to $2\theta = 70°$ ($\sin \theta_{max}/\lambda = 0 \cdot 807$ Å^{-1}) with a constant scan rate of $3°$ min^{-1}, scan range from $1 \cdot 0°$

---

* Dibenzo[*ij,uv*]|1,4,7,13,16,19|hexaoxacyclotetracosane-25,26-dicarboxylic acid.

Table 1. *Crystal data for* bis(2'-carboxy-1',3'-xylyl)-24-crown-6 *at* 113 K

Molecular formula: $C_{26}H_{32}O_{10}$, $M_r = 504.54$, m.p. 486–487 K
Orthorhombic, space group *Ccca*

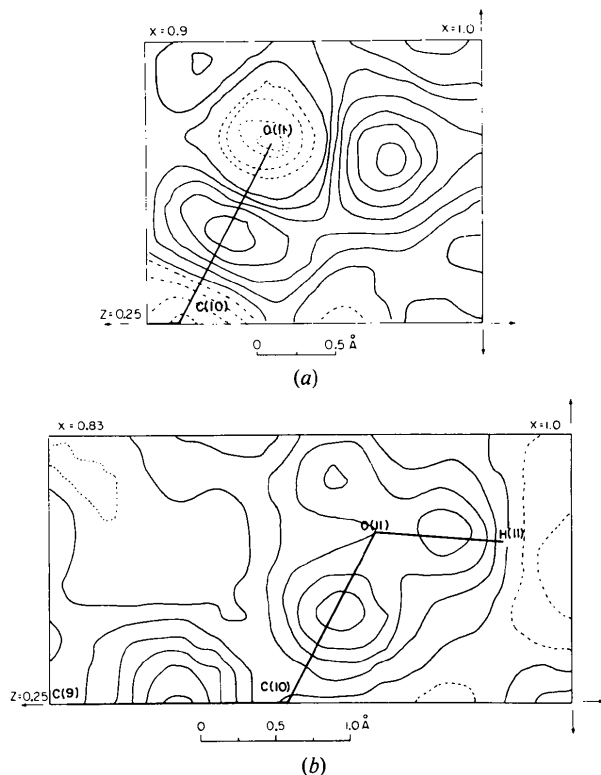|	
$a = 21.405$ (5) Å	$Z = 4$
$b = 12.925$ (2)	$F(000) = 1072$
$c = 8.878$ (3)	$D_c = 1.364$ Mg m^{-3}
$V = 2456.2$ Å^3	$\mu(Mo\ K\alpha) = 0.1$ mm^{-1}

(a)

(b)

Fig. 1. Two $x, \frac{1}{4}, z$ sections of difference syntheses near the plane of the carboxyl group: (a) location of the hydroxy H atom at an intermediate stage of refinement, (b) X–X deformation map after the final refinement (see text). Contour lines are drawn at intervals of 0.05 e Å^{-3}, negative contour lines being broken.

Table 2. *Atomic fractional coordinates and isotropic thermal parameters*

E.s.d.'s are given in parentheses in units of the last decimal place.

	x	y	z	U_{eq}/U (Å^2)
O(1)	1.00	1.0326 (1)	0.25	0.014
C(2)	0.95604 (6)	1.0955 (1)	0.3268 (2)	0.018
C(3)	0.91567 (7)	1.0297 (1)	0.4278 (2)	0.020
O(4)	0.87646 (5)	0.9654 (1)	0.3379 (1)	0.016
C(5)	0.83853 (6)	0.9024 (1)	0.4327 (2)	0.018
C(6)	0.80556 (6)	0.8232 (1)	0.3373 (2)	0.016
C(7)	0.74017 (6)	0.8233 (1)	0.3334 (2)	0.021
C(8)	0.70755 (8)	0.75	0.25	0.023
C(9)	0.83849 (7)	0.75	0.25	0.014
C(10)	0.90885 (7)	0.75	0.25	0.014
O(11)	0.93712 (4)	0.7493 (1)	0.3762 (1)	0.018
H(2a)	0.9301 (7)	1.134 (1)	0.251 (2)	0.026 (4)
H(2b)	0.9785 (8)	1.146 (1)	0.390 (2)	0.023 (4)
H(3a)	0.8908 (8)	1.074 (1)	0.494 (2)	0.028 (4)
H(3b)	0.9408 (8)	0.990 (1)	0.496 (2)	0.032 (5)
H(5a)	0.8082 (7)	0.944 (1)	0.486 (2)	0.026 (4)
H(5b)	0.8656 (7)	0.869 (1)	0.510 (2)	0.024 (4)
H(7)	0.7176 (8)	0.874 (1)	0.390 (2)	0.029 (5)
H(8)	0.6624 (11)	0.75	0.25	0.026 (6)
H(11)	0.9756 (13)	0.755 (3)	0.367 (3)	0.022 (9)

heavy-atom model was refined to $R = 0.09$. At this stage all the H atoms were located on difference maps. The delocalized hydroxyl H atom was found to be situated in a general position (Fig. 1), which indicated that in the crystal this H atom undergoes rapid oscillations between the two carboxyl substituents.

Full-matrix least-squares anisotropic refinement of the nonhydrogen and isotropic refinement of the H atoms gave a final $R = 0.043$ ($R = 0.056$ for all non-zero reflections). Parameters of the H atoms were adjusted only with low-order data, $\sin \theta/\lambda \le 0.55$ Å^{-1}. At convergence the final goodness-of-fit was 1.45. The quantity minimized was $\Sigma w(\Delta F)^2$, where $w = 1/\sigma^2(F_o)$. Form factors for C and O were taken from *International Tables for X-ray Crystallography* (1974), those for H from Stewart, Davidson & Simpson (1965). In the final difference map the highest peak and deepest trough were 0.2 and 0.1 e Å^{-3}, respectively.

To improve the positional parameters of the atomic nuclei of C and O, additional refinement was carried out with two different weighting schemes: (a) $w(F_o) = \exp(7 \sin^2 \theta/\lambda^2)/\sigma^2(F_o)$ for all data (Dunitz & Seiler, 1973), and (b) $w(F_o) = 0$ for reflections with $\sin \theta/\lambda < 0.50$ Å^{-1} and $w(F_o) = 1/\sigma^2(F_o)$ for 1098 observations with $\sin \theta/\lambda \ge 0.50$ Å^{-1}. H atom parameters were not optimized in this process. The agreement values were $R_a = 0.048$, and $R_b = 0.045$ (g.o.f. = 1.08). While the final atomic positions are very similar in refinements (a) and (b), each set is markedly different from the coordinates previously derived with an unmodified experimental weighting scheme. This is reflected mainly in a significant increase ($>3\sigma$) of the C(2)–C(3) and C(7)–C(8) lengths (Table 3). In close correlation, the

below $K\alpha_1$ to 1.0° above $K\alpha_2$, and stationary background measurements at the beginning and end of each scan. Three intensity-control reflections, monitored after each group of 97 measurements, showed no decay of the crystal. Data were corrected for Lorentz and polarization effects, but not for absorption or secondary extinction.

The structure was solved by weighted-tangent-formula refinement (*MULTAN* 74; Main, Woolfson, Lessinger, Germain & Declercq, 1974) applied to 220 reflections with $|E| \ge 1.75$. All non-hydrogen atoms, including those located on special positions, were found in the best E map. Subsequent refinement was based on 1660 observations above threshold, $F_o^2 \ge 3\sigma(F_o^2)$. The

Table 3. *Bond distances* (Å)

Final bond distances were derived from coordinates of the high-angle refinement (see text). For comparison, bond lengths obtained in refinements with (a) $w = 1/\sigma^2(F_o)$ and (b) $w = \exp(7\sin^2\theta/\lambda^2)/\sigma^2(F_o)$ for all data are listed as well.

		(a)	(b)
O(1)—C(2)	1·418 (2)	1·420 (1)	1·418 (1)
C(2)—C(3)	1·508 (2)	1·498 (2)	1·503 (2)
C(3)—O(4)	1·425 (2)	1·428 (2)	1·422 (2)
O(4)—C(5)	1·425 (2)	1·423 (2)	1·422 (2)
C(5)—C(6)	1·505 (2)	1·503 (2)	1·504 (2)
C(6)—C(7)	1·400 (2)	1·402 (2)	1·401 (2)
C(6)—C(9)	1·411 (2)	1·407 (1)	1·411 (1)
C(7)—C(8)	1·390 (2)	1·383 (2)	1·388 (2)
C(9)—C(10)	1·506 (2)	1·508 (2)	1·506 (2)
C(10)—O(11)	1·274 (1)	1·271 (1)	1·271 (1)

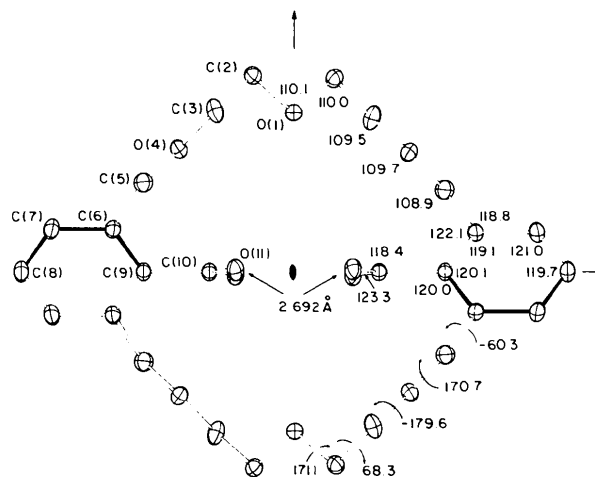| C(2)—H(2a)	1·00 (2)	C(5)—H(5b)	1·00 (2)
C(2)—H(2b)	0·98 (2)	C(7)—H(7)	0·96 (2)
C(3)—H(3a)	0·98 (2)	C(8)—H(8)	0·97 (2)
C(3)—H(3b)	0·96 (2)	O(11)—H(11)	0·83 (3)
C(5)—H(5a)	0·97 (2)		

Fig. 2. A perspective drawing of the molecular structure showing the numbering. Thermal ellipsoids correspond to 50% probability. E.s.d.'s of the bond and torsion angles are 0·1°. The value of −60·3° refers to the O(4)—C(5)—C(6)—C(9) torsion angle.

underweighting of low-order observations in refinements (a) and (b) led to smaller parameters of thermal motion. For example, on the assignment of zero weights to 562 reflections below $\sin\theta/\lambda = 0\cdot50$ Å^{-1} the refined parameters of the average squared amplitude of vibration were reduced by $11 \pm 2\%$. The discussion which follows is based on results from the high-angle refinement. Final atomic coordinates are presented in Table 2. Bond distances obtained from calculations with the different weighting schemes are compared in Table 3.*

In a final stage the refined positions of the H atoms were modified to make all C—H and O—H distances equal respectively to 1·08 and 0·98 Å, and several difference maps were computed in various sections of the asymmetric unit. All F_o values above threshold (1660 observations) were used for this synthesis. The F_c values were based on parameters refined with high-angle data for C and O, and on the calculated positions for H. (In fact, one additional cycle of refinement was carried out with the modified H positions held constant; however, the resulting changes in positional and vibrational parameters of the non-hydrogen atoms were mostly insignificant.) The seven highest peaks found on these maps (0·21–0·30 e Å^{-3}) are centered on the C—C and carboxyl C—O (Fig. 1) bonds in the molecule. Lower peaks (0·13–0·20 e Å^{-3}) were observed along other C—O bonds and some of the C—H bonds, as well as close to the O atom nuclei (very diffuse). The e.s.d. in the calculated Fourier synthesis is

0·02 e Å^{-3}. Similar features were observed in previous low-temperature studies of crown compounds (Goldberg, 1975). However, they appear significantly more prominent in a recent analysis of 18-crown-6 at 100 K (Maverick, Seiler, Schweizer & Dunitz, 1980).

Discussion of results

The present study provides an example of a dicarboxylic acid whose crystal structure consists of discrete molecules held together by weak van der Waals forces. The bis(2'-carboxy-1',3'-xylyl)-24-crown-6 species has D_2 symmetry, occupying the (222) special positions in the unit cell. Fig. 2 shows one view of the molecule with the atom numbering. In the observed conformation all polar groups are hidden within the macrocycle and covered by a lipophilic skin of C—H bonds. The carboxyl substituents form an intramolecular cyclic pair of O—H···O hydrogen bonds. These interactions involve crystallographically equivalent donor and acceptor O atoms; therefore, they belong to the class of symmetric or symmetry-restricted hydrogen bonds (Ichikawa, 1978). Correspondingly, the carboxy dimer has a disordered structure, all C—O bonds being equal in length. Since the refined thermal parameters of O(11) are relatively small, trace $U = 0\cdot054$ Å^2, the disorder is believed to be dynamic. If the disorder were completely static, representation of both the hydroxyl and the carbonyl O atom positions (which are approximately 0·3 Å from each other) by a single set of atomic coordinates would result in an artificially high temperature factor (Leiserowitz, 1976). As mentioned above, a difference map (Fig. 1) indicates that the

hydroxy H atoms are oscillating between the two carboxy groups. Indeed, an attempt to situate these protons in refinement on the centered twofold axis at $1,\frac{3}{4},z$ induced a very large parameter of motion for H(11). The dimensions of the hydrogen bonds are: C(10)–O(11) = 1·274 (1), O(11)–H(11) = 0·83 (3), O(11) (at x,y,z)···O(11') (at $2 - x, \frac{3}{2} - y, z$) = 2·692 (1) Å, C(10)–O(11)–H(11) = 113 (2), C(10)–O(11)···O(11') = 118·4 (1) and O(11)–H(11)···O(11') = 169 (3)°. These results are similar to previously observed geometries of *inter*molecular carboxy dimers in crystals of mono- and dicarboxylic acids (Leiserowitz, 1976).

Bond distances listed in Table 3 correlate well with those found at 113 K in BACR5 (Goldberg, 1976) and BAPCR5 (Goldberg & Rezmovitz, 1978), and at room temperature in other 2,6-disubstituted benzoic acids (Benghiat & Leiserowitz, 1972). A significant exception refers to dimensions of the carboxy group which is ideally disordered only in the present example. Bond lengths in the benzene moiety range from 1·390 Å for the peripheral bonds to 1·411 Å for bonds adjacent to the electron-withdrawing COOH group. The C(sp^3)–O (1·418 and 1·425 Å) and C(sp^3)–C(sp^3) (1·508 Å) distances follow the trends usual for crown ether compounds. Bond and torsion angles are shown in Fig. 2. Energetically optimal values are attained for all conformational parameters of the aliphatic fragment; the torsion angles about C–O bonds are antiplanar, those about C–C bonds are synclinal. The aromatic rings are planar within $\pm0\cdot01$ Å. As in related 2,6-disubstituted benzoic acids the plane of the carboxyl group is rotated with respect to the plane of the phenyl ring. The angle of twist in the present structure is 52°, compared to 59° in BACR5 (Goldberg, 1976), 57° in BAPCR5 (Goldberg & Rezmovitz, 1978), 53° in 2,6-dimethylbenzoic acid (Anca, Martinez-Carrera & Garcia-Blanco, 1967) and 48° in 2,4,6-trimethylbenzoic acid (Benghiat & Leiserowitz, 1972). The angle between the mean planes of the two transannularly located phenyl rings is 103°. The potential dipole–dipole interaction between nucleophilic O(4) and electrophilic C(10) seems to be much less pronounced than the corresponding O(ring)···C=O interactions in BAPCR5 and BACR5; the indicative mean O···C distances in the three compounds are 2·97, 2·86 and 2·76 Å, respectively. This appears to be mainly due to a reduced electrophilicity of C(10) as a result of the disorder in carboxy groups, and the dominant function of the interaction of hydrogen bonding. All bond angles within the aliphatic fragment are confined to the small range 108·9–110·1°, in disagreement with previous observations. Pickett & Strauss (1970) suggested that in saturated oxanes the C–O–C bond angle is expected to be larger than the O–C–C bond angle. Indeed, in crown ether moieties characterized by a favorable conformation most of the observed O–C–C angles are

Table 4. *Analysis of thermal motion*

(*a*) Differences in the mean-square vibration amplitudes of bonded atoms along the lines between them

O(1)–C(2)	6 Å² × 10⁻⁴	C(6)–C(7)	0 Å² × 10⁻⁴
C(2)–C(3)	1	C(6)–C(9)	10
C(3)–O(4)	3	C(7)–C(8)	2
O(4)–C(5)	21	C(9)–C(10)	11
C(5)–C(6)	1	C(10)–O(11)	15

(*b*) Rigid-body motion. The components of the tensors are referred to the Cartesian crystal axes. The dimensions of L_{ii}, T_{ii} and S_{ii} are rad² × 10⁻⁵, Å² × 10⁻⁴ and rad Å × 10⁻⁴, respectively.

(1) The entire molecule (36 atoms)

L_{11}	44 (8)	T_{11}	130 (6)	S_{11}	−1 (1)
L_{22}	62 (5)	T_{22}	187 (7)	S_{22}	4 (1)
L_{33}	0 (4)	T_{33}	113 (11)	S_{33}	−3

$$\langle(\Delta U)^2\rangle^{1/2} = 0\cdot0031 \text{ Å}^2, \text{ weighted } R = 0\cdot20.$$

The eigenvalues of the molecular tensor of inertia along **a**, **b** and **c** are 247, 437 and 615 at. wt Å², respectively.

(2) The 28-atom fragment excluding C(3), O(11) and their symmetry-equivalents

L_{11}	55 (6)	T_{11}	121 (4)	S_{11}	−2 (1)
L_{22}	70 (4)	T_{22}	150 (5)	S_{22}	5 (8)
L_{33}	12 (3)	T_{33}	93 (9)	S_{33}	−3

$$\langle(\Delta U)^2\rangle^{1/2} = 0\cdot0019 \text{ Å}^2, \text{ weighted } R = 0\cdot12.$$

close to tetrahedral, while the C–O–C angles are usually about 2–3° larger (Goldberg, 1980). No reasonable explanation of the deviation from this trend in the present study can be offered. However, one may still conclude that the overall molecular structure of the title compound is characterized by nearly optimal geometric parameters, in close correlation with the fact that there exists an excellent fit between the size of the 24-membered macrocycle and the dimensions of a carboxy dimer incorporated into it.

An analysis of the vibrational tensors of C and O was carried out with *TMA* (Shmueli, 1972). Initially, we examined the differences in the mean-square vibration amplitudes of bonded atoms along the lines between them. For eight bonds these differences are small ($\leq0\cdot0011$ Å²). For the two remaining bonded pairs O(4)–C(5) (0·0021 Å²) and C(10)–O(11) (0·0015 Å²) they exceed, however, twice their e.s.d.'s. According to Hirshfeld (1976) this may indicate that the temperature factors obtained from the present refinement are affected to some extent by experimental errors.

The observed thermal parameters have subsequently been fitted to general rigid-body motions described by **T**, **L** and **S** tensors. The main results of this calculation are given in Table 4. The overall thermal motion of the molecule seems to be anisotropic and mainly translational; the square amplitudes of translation along the molecular axes of inertia are 0·013, 0·019 and

$0 \cdot 011$ Å^2. Librational vibrations at 113 K are small (maximum amplitude about $1 \cdot 4°$). Because of symmetry constraints the three axes of libration pass through the molecular center and run parallel to the unit-cell vectors. When the entire heavy-atom framework is taken as a rigid body, the agreement between the observed and calculated U^{ij} is rather poor. The root-mean-square discrepancy of ΔU^{ij} is $0 \cdot 0031$ Å^2, which is large compared with the mean e.s.d. of the observed U^{ij} ($0 \cdot 0005$ Å^2). Therefore, the rigid-body model seems to be incompatible with the observed atomic vibrations. A particularly poor agreement is between the observed and calculated U^{ij} values of C(3) and O(11). As suggested by the shape and orientation of the ellipsoid of C(3), this atom exhibits excessive torsional vibration in a direction perpendicular to the plane of the C(2)—C(5) fragment (Fig. 2); the vibration components of C(2), C(3), O(4) and C(5) along this direction are $0 \cdot 017$, $0 \cdot 028$, $0 \cdot 018$ and $0 \cdot 018$ Å^2, respectively. Similarly, the respective vibration components of C(9), C(10) and O(11) along the normal to the plane of the carboxyl group are $0 \cdot 016$, $0 \cdot 015$ and $0 \cdot 023$ Å^2, indicating that thermal motion of O(11) is somewhat independent. When C(3) and O(11) along with their symmetry-equivalents were excluded from the calculation, the value of the r.m.s. ΔU^{ij} dropped to $0 \cdot 0019$ Å^2. In comparison with the entire molecule, the overall thermal motion of the remaining 28-atom fragment can be described by slightly larger librations and smaller translations (Table 4). The invalidity of the rigid-body model is also reflected in the fact that differences between the mean-square vibration amplitudes of non-bonded atoms along their interatomic vectors are large. In the non-bonded pairs involving C(3) some of these differences exceed $0 \cdot 01$ Å^2. The bond lengths presented in Table 3 are not corrected for the effects of thermal motion. While possible corrections for the apparent librations are expected to be small ($\leq 0 \cdot 001$ Å), the influence of internal vibrations on the molecular geometry is unknown.

The packing of the molecules is shown in Fig. 3. The four molecules in the unit cell occupy special positions at the intersections of three twofold axes $(0, \frac{1}{4}, \frac{3}{4}; 0, \frac{3}{4}, \frac{1}{4}; \frac{1}{2}, \frac{3}{4}, \frac{3}{4}; \frac{1}{2}, \frac{1}{4}, \frac{1}{4})$. All intermolecular distances are longer than or approximately equal to the sums of the corresponding van der Waals radii. However, two types
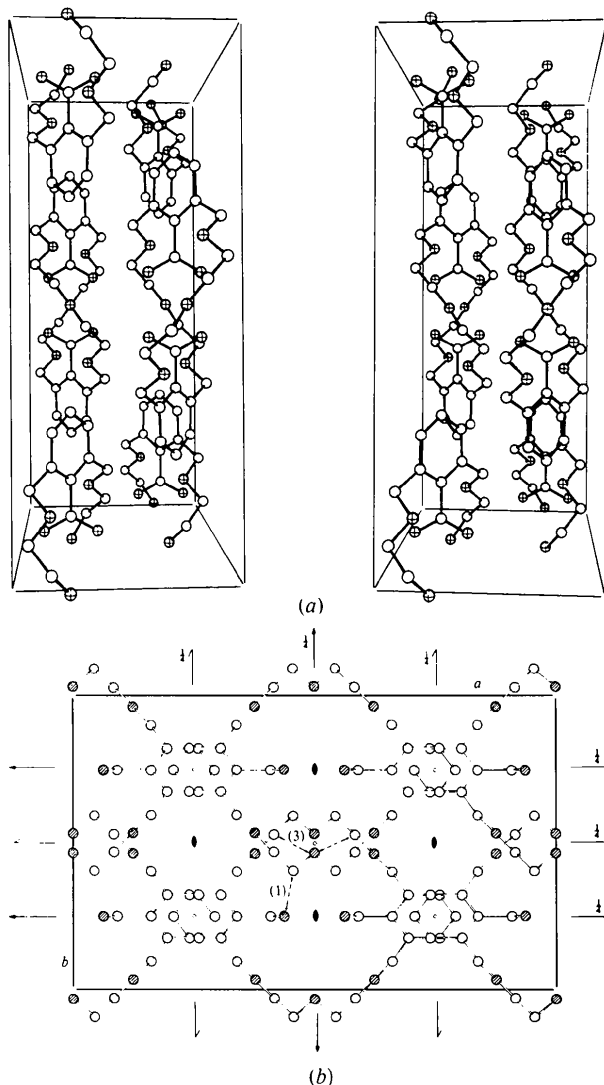

(a)

(b)

Fig. 3. An illustration of the crystal structure. (a) Stereoscopic view along a direction slightly tilted to **b**. (b) Parallel projection down **c**, showing two of the intermolecular C—H···O interactions described in Table 5: (1) $3 \cdot 327$ and (3) $3 \cdot 477$ Å. Symbols of some of the symmetry elements are marked.

of specific interactions seem to be particularly important. The crystal structure can be described as composed of sheets of different molecular fragments perpendicular to **a**. Sheets comprising the aromatic groups, which are centered at $x = \frac{1}{4}$ and $x = \frac{3}{4}$, alternate with sheets containing the aliphatic and carboxyl moieties centered at $x = 0$ and $x = \frac{1}{2}$. The phenyl rings of adjacent molecules displaced along **a** (e.g. those located at $0, \frac{3}{4}, \frac{1}{4}; \frac{1}{2}, \frac{3}{4}, \frac{3}{4}; 1, \frac{3}{4}, \frac{1}{4}$) are parallel to and overlap each other. Thus, each ring is effectively in close packing with two neighbors located about $3 \cdot 47$ Å below and above its mean plane. In layers perpendicular to **a** the molecules are held together by arrays of C—H···O attractions, with O(1) and O(11) acting as

Table 5. *Geometry of intermolecular* C—H···O *interactions*

C^i—O···H—C^p	O···H (Å)	O···C^p (Å)	O···H—C^p (°)	C^i—O···C^p (°)
(1) C(10)—O(11)···H(2b)—C(2) (i)	2·62 (2)	3·327 (2)	129 (1)	139·4 (1)
(2) C(10)—O(11)···H(3a)—C(3) (i)	2·73 (2)	3·361 (2)	123 (1)	113·4 (1)
(3) C(2)—O(1)···H(3b)—C(3) (ii)	2·60 (2)	3·477 (2)	151 (2)	100·6 (1)

Symmetry code: (i) $x, y - \frac{1}{2}, 1 - z$; (ii) $2 - x, 2 - y, 1 - z$ and $x, 2 - y, z - \frac{1}{2}$.

acceptor sites (Fig. 3 and Table 5). While on one side the carboxy O atom is shielded from intermolecular interactions by the crown ether ring, it is involved in relatively short contacts in the opposite direction. Relevant nonbonding distances include: $O(11)\cdots C(5)$ = 2·936 (2) and $O(11)\cdots O(4)$ = 3·098 (2) within the asymmetric unit, and $O(11)\cdots C(2)$ = 3·327 (2) and $O(11)\cdots C(3)$ = 3·361 (2) Å between neighboring molecules. It appears that the observed least-energy conformation of the crown ether is well accommodated by inter- as well as intramolecular van der Waals interactions.

The present structure provides a rare example of a non-rigid macrocyclic species whose geometry in the crystal is characterized by a very high organization. Moreover, it suggests that crown ether ligands which are known for their remarkable ability to form complexes with various molecules and ions, may also be useful in hosting and enhancing interactions between other functional moieties.

References

ANCA, R., MARTÍNEZ-CARRERA, S. & GARCÍA-BLANCO, S. (1967). *Acta Cryst.* 23, 1010–1016.

BENGHIAT, V. & LEISEROWITZ, L. (1972). *J. Chem. Soc. Perkin Trans.* 2, pp. 1778–1785.

DUNITZ, J. D. & SEILER, P. (1973). *Acta Cryst.* B29, 589–595.

GOLDBERG, I. (1975). *Acta Cryst.* B31. 754–762, 2592–2600.

GOLDBERG, I. (1976). *Acta Cryst.* B32, 41–46.

GOLDBERG, I. (1980). *The Chemistry of Ethers, Crown Ethers, Hydroxyl Groups and their Sulphur Analogs*, Supplement E1, edited by S. PATAI, pp. 175–214. London: John Wiley.

GOLDBERG, I. & REZMOVITZ, H. (1978). *Acta Cryst.* B34, 2894–2896.

HIRSHFELD, F. L. (1976). *Acta Cryst.* A32, 239–244.

ICHIKAWA, M. (1978). *Acta Cryst.* B34, 2074–2080.

International Tables for X-ray Crystallography (1974). Vol. IV, pp. 71–98. Birmingham: Kynoch Press.

LEISEROWITZ, L. (1976). *Acta Cryst.* B32, 775–802.

MAIN, P., WOOLFSON, M. M., LESSINGER, L., GERMAIN, G. & DECLERCQ, J. P. (1974). *MULTAN 74. A System of Computer Programs for the Automatic Solution of Crystal Structures from X-ray Diffraction Data*. Univs. of York, England, and Louvain. Belgium.

MAVERICK, E., SEILER, P., SCHWEIZER, W. B. & DUNITZ, J. D. (1980). *Acta Cryst.* B36, 615–620.

PICKETT, H. M. & STRAUSS, H. L. (1970). *J. Chem. Phys.* 53. 376–388.

SHMUELI, U. (1972). *TMA. Thermal Motion Analysis*, Department of Chemistry, Tel-Aviv Univ., Tel-Aviv.

STEWART, R. F., DAVIDSON, E. R. & SIMPSON, W. T. (1965). *J. Chem. Phys.* 42, 3175–3187.

STROUSE, C. E. (1976). *Rev. Sci. Instrum.* 47, 871–876.

The Structure of the 1:2 Complex 4,4-Diethylmorpholinium 7,7,8,8-Tetracyanoquinodimethanide, DEM(TCNQ)₂, at 294 K

BY HANS MORSSINK AND BERT VAN BODEGOM

Laboratorium voor Chemische Fysica, Materials Science Center, Rijksuniversiteit Groningen, Nijenborgh 16, 9747 AG Groningen, The Netherlands

Abstract

$C_8H_{18}NO^+.2C_{12}H_4N_4^{-1/2}$, DEM(TCNQ)₂, is triclinic, space group $P\bar{1}$, with a = 7·902 (4), b = 28·134 (6), c = 7·514 (3) Å, α = 91·26 (2), β = 118·47 (4), γ = 93·67 (2)°, U = 1462 Å³, Z = 2; d_c = 1·255, d_m = 1·253 Mg m⁻³. Final $R_w(F)$ = 0·077 for 5460 independent reflections. The structure consists of two types of TCNQ sheets, A and B, parallel to (010) with DEM molecules placed between these sheets. In the sheets of type A, TCNQ molecules united into dimers form a two-dimensional array. The intradimer separation is 3·41 (1) Å; the perpendicular interdimer separation is 3·19 (1) Å for units along [101] and [001]. The intradimer overlap is of the shifted ring–ring type. In the type B sheets, TCNQ units form dimerized